

# Cosmic microwave background anisotropy data correlation in WMAP and Relikt-1 experiments

D P Skulachev

DOI: 10.3367/UFNe.0180.201004c.0389

## Contents

1. Introduction	373
2. The WMAP data used in the analysis	373
3. The ‘cold spot’	373
4. Dipole component	374
5. Higher anisotropy components	374
6. Signal detected by Relikt-1	374
7. Method of the signal structure study	374
8. Analysis of mutual covariance	375
9. Single-frequency measurements	375
10. Conclusions	375
References	376

**Abstract.** A comparison is made of cosmic microwave background anisotropy data obtained from the WMAP satellite in 2001–2006 and from the Relikt-1 satellite in 1983–1984. It is shown that the low-temperature area found by Relikt-1 is the location of the ‘coldest spot’ of the WMAP radiomap. The mutual correlation of the two datasets is estimated and found to be positive for all sky regions surveyed. The conclusion is made that with the 98% probability, the Relikt-1 experiment had detected the same signal that was later identified by WMAP. A discussion is given of whether the Relikt-1 experiment parameters were chosen correctly.

## 1. Introduction

The anisotropy of cosmic microwave background (CMB) radiation was discovered in sky surveys carried out by dedicated artificial satellites [1, 2]. By the middle of 2009, the CMB has been explored by three space experiments: Relikt-1 (USSR, 1983–1984), COBE (Cosmic Background Explorer) (USA, 1989–1993), and WMAP (Wilkinson Microwave Anisotropy Probe) (USA, launched in 2001). In May 2009, the Planck European space mission with a similar research task was successfully launched.

The sensitivity of the Relikt-1 experiment was limited by the technical capabilities of that time and can be considered rather modest according to modern criteria. However, that

sensitivity proved to be sufficient to discover and measure the CMB anisotropy parameters. The dipole anisotropy was detected and the amplitude of the quadrupole anisotropy for a given perturbation spectrum was measured [3]. A low-temperature area—a ‘cold spot’—was found on the sky radiomap [1]. The measurements were carried out only at one frequency and on the verge of the sensitivity limit, and therefore the results obtained needed to be confirmed by more precise measurements.

The American satellite COBE was launched six years after Relikt-1 with better equipment. Estimates of the dipole and quadrupole anisotropy for a given spectrum obtained by both satellites were found to be consistent within error. The cold spot found by Relikt-1 was not confirmed by COBE [4, 5], but the signal-to-noise ratio on the COBE radiomap was rather low in this area of the sky.

Results of any observations can be reliably confirmed or rejected only by analyzing independent experimental data with a good signal-to-noise ratio. At present, such data has been obtained by the WMAP satellite during five years of continuous measurements [6]. In what follows, we present the results of a comparison of the WMAP and Relikt-1 experimental data.

## 2. The WMAP data used in the analysis

The central frequency of the Ka and Q channels of the WMAP satellite coincides with the working frequency of the Relikt-1 radiometer, and we therefore use the brightness temperatures in the Ka and Q channels of the WMAP satellite for the subsequent analysis.

## 3. The ‘cold spot’

Figure 1 shows a part of the WMAP radiomap in ecliptic coordinates. The data was smoothed with an angular

D P Skulachev Space Research Institute, Russian Academy of Sciences, ul. Profsoyuznaya 84/32, 117997 Moscow, Russian Federation  
Tel. (7-495) 333 43 22. E-mail: dskulach@mx.iki.rssi.ru

Received 22 June 2009

Uspekhi Fizicheskikh Nauk 180 (4) 389–392 (2010)

DOI: 10.3367/UFNe.0180.201004c.0389

Translated by K A Postnov; edited by A M Semikhatov

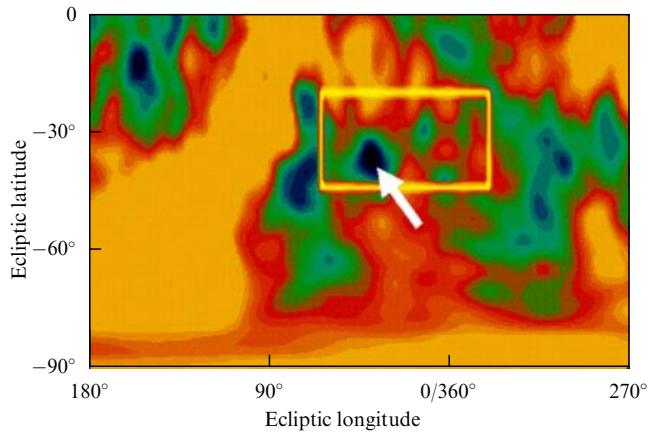


**Figure 1.** The ‘Spot’ of WMAP (marked with the arrow) and the ‘cold’ spot area of Relikt-1 (inside the white quadrangle).

resolution of  $15^\circ$ . The brightness temperature of regions near the galactic plane is conventionally set to zero. The dark color marks low-temperature areas. The white quadrangle shows the area where Relikt-1 found the coldest spot. The coordinates of the quadrangle are taken from [1].

It can be seen that several cold points fall within the area shown, with one of them (marked by the arrow in Fig. 1) being the famous ‘Spot,’ the coldest spot on the entire WMAP radiomap [1]. The Spot has ecliptic coordinates  $\lambda = 39^\circ$ ,  $\beta = -37^\circ$  and galactic coordinates  $l = 209^\circ$ ,  $b = -57^\circ$ . The low-temperature area on the Relikt-1 map was singled out using additional data averaging. In this procedure, cold points apparently joined together into a single big spot, which was actually discovered. The parameters of the measured brightness temperature minimum are given in [1]. The exact location of the spot itself was not then measured due to a high noise level, which is why an extended area inside the quadrangle was marked.

We note that a part of the cold area on the Relikt-1 radiomap near zero ecliptic longitudes has the brightness temperature close to zero on the WMAP sky map. Supposedly, it is exactly this region that was studied in [4, 5], where it was concluded that the Relikt-1 data are inconsistent with the COBE data. However, the list of the coldest spots on the COBE sky map [8] does not include the Spot itself, the coldest object later discovered by WMAP.

#### 4. Dipole component

The CMB dipole component parameters determined from the WMAP data [9] and the Relikt-1 data [3] are given in Table 1. The errors correspond to a 90% confidence level. Thermodynamic values of the brightness temperature are used.

Table 1 shows that the results of two experiments are consistent within errors. A small (about 6%) difference in the dipole amplitude can be explained by a systematic calibration error of the Relikt-1 radiometer.

**Table 1.** Estimate of the dipole CMB anisotropy.

Experiment	Dipole component	
	Amplitude	Galactic coordinate of the maximum
WMAP	$3.358 \pm 0.017$ mK	$l = 263.86^\circ \pm 0.04^\circ$ , $b = 48.24^\circ \pm 0.1^\circ$
Relikt-1	$3.16 \pm 0.12$ mK	$l = 267.1^\circ \pm 3^\circ$ , $b = 48.6^\circ \pm 3^\circ$

#### 5. Higher anisotropy components

In the Relikt-1 data, the amplitudes of higher anisotropy harmonics were found by statistical modeling under the assumption of the Harrison–Zeldovich primordial perturbation spectrum. An estimate is given for the rms value of the quadrupole component ( $Q_{\text{rms-ps}}$ ) for this spectrum [1].

In the WMAP data, the quadrupole component was determined as [10]

$$Q_{\text{rms-ps}} = \sqrt{\frac{5C_2}{4\pi}}, \quad (1)$$

with  $C_2$  calculated as

$$C_2 = \frac{2\pi}{6} \sum_{l=2}^{15} \frac{C_l l(l+1)/2\pi}{14}, \quad (2)$$

where  $C_l l(l+1)/2\pi$  is the  $l$ th component of the anisotropy power spectrum [11]. The summation limits here approximately correspond to the transfer function of the Relikt-1 radiometer, taking smoothing into account. The averaging over  $l$  in formula (2) is used to reduce uncertainties in the estimate of  $C_2$ , taking into account that  $C_l l(l+1)$  is independent of  $l$  for the Harrison–Zeldovich spectrum.

The corresponding values (in microkelvins) are presented in Table 2. For Relikt-1, a 90% confidence level for the interval is given.

**Table 2.** Estimates of higher-anisotropy components.

Experiment	Quadrupole component $Q_{\text{rms-ps}}$
WMAP	18.9 $\mu$ K
Relikt-1	16.5–90 $\mu$ K

It follows from Table 2 that the data of both experiments are consistent within errors.

We note that the values in Table 2 give model-dependent estimates of the entire anisotropy and not the measured quadrupole amplitudes. The measured quadrupole amplitudes would be such if the measured anisotropy were generated by primordial fluctuations with the Harrison–Zeldovich spectrum.

#### 6. Signal detected by Relikt-1

Although the anisotropy estimates made by Relikt-1 are confirmed by the WMAP data, this could be considered purely coincidental because the spectrum and the form of the signal discovered by Relikt-1 have not actually been determined. The anisotropy was calculated in [1] from the dispersion analysis using a small excess of measured values against pure noise, and it is not at all clear whether such an excess is due to a real signal or to quite different reasons, e.g., electric interference or external radiation. Therefore, a more detailed study of the structure of the signal measured by Relikt-1 is in order.

#### 7. Method of the signal structure study

Studying the Relikt-1 signal structure directly is impossible due to a poor signal-to-noise ratio. In contrast to Relikt-1, the WMAP data have low noise, which allows reliably analyzing

the mutual covariance of the Relikt-1 and WMAP data. If the covariance were small or had an alternate sign, it would have to be recognized that the signal detected by Relikt-1 is unrelated to the radio emission from the observed area of the sky, i.e., the results of Relikt-1 are erroneous.

### 8. Analysis of mutual covariance

The radiomap of the sky in the Relikt-1 experiment was constructed from individual scans that represent big sweeps of the celestial sphere [12]. For the subsequent analysis, 14 Relikt-1 scans were selected, which amount to 80% of the available observational data. Exactly the same scans were selected from the WMAP data [13]. The selected data for both experiments were averaged with an angular resolution of 15° and then compared to each other.

The mutual covariance COV of the WMAP and Relikt-1 data in each scan was calculated as

$$COV = \frac{1}{\sqrt{\sum W(i)}} \text{sign} \left( \sum T_{WMAP}(i) T_{Rel}(i) \right) \times \sqrt{\text{abs} \left( \sum T_{WMAP}(i) T_{Rel}(i) W(i) \right)}, \quad (3)$$

where  $T_{WMAP}(i)$  is the brightness temperature at the  $i$ th point of the WMAP scan,  $T_{Rel}(i)$  is the brightness temperature at the  $i$ th point of the Relikt-1 scan,  $W(i) = 1/N^2(i)$  is the statistical weight of the  $i$ th point, and  $N(i)$  is the noise level at the  $i$ th point of the Relikt-1 scan. The summation ranges over all points in a scan. The statistical weight of points located within  $\pm 20^\circ$  of the galactic plane is zero. The WMAP noise is ignored because it can be neglected in comparison with that of Relikt-1.

The results are shown in Fig. 2, in where the mutual covariance is plotted versus the scan number. Line 1 shows the level of the mutual covariance of the WMAP and Relikt-1 data for each scan. Line 2 shows the effective rms of the signal measured by WMAP in each scan.

It follows from Fig. 2 that the covariance of the WMAP and Relikt-1 data is positive for all scans. The intensity of the correlated signal is close to the WMAP signal. In principle, this could be possible in the absence of a signal due to pure statistical noise fluctuations on the Relikt-1 map. But the statistical modeling shows that the probability of such a

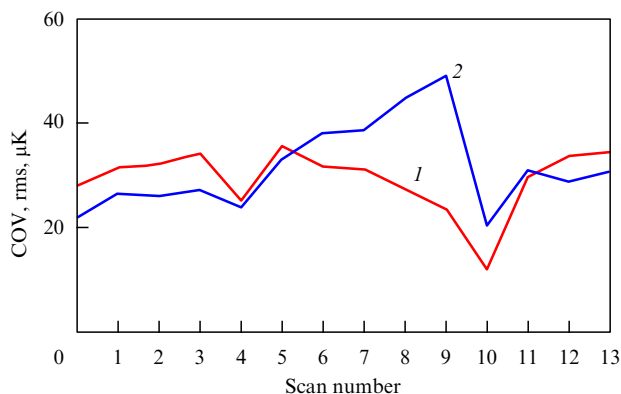


Figure 2. The mutual covariance of the WMAP and Relikt-1 data (1) and the effective rms WMAP signal (2).

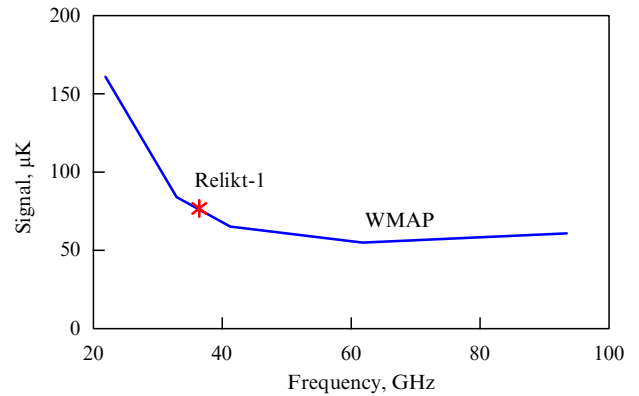


Figure 3. The spectrum of the signal measured by WMAP. The asterisk shows the working frequency of Relikt-1.

situation is less than 2%. Cutting the cold spot from the analysis leaves the result virtually unchanged.

### 9. Single-frequency measurements

WMAP radiometers operate in the five frequency bands covering the frequency range from 20 to 106 GHz. It is well known that the thermodynamic temperature of CMB is independent of its frequency. However, in addition to the CMB signal, the radiometers measure diffuse radio (bremsstrahlung and synchrotron) emission of interstellar gas and thermal radiation from dust. The spectra of these additional sources are known (with a certain accuracy), which allows detecting the CMB signal anisotropy against their background (also with a certain accuracy).

The WMAP signal is plotted as a function of frequency in Fig. 3. The data, as previously, are averaged with an angular resolution of 15° and relate to regions far outside the galactic plane. The increase at low frequencies is due to a contribution from thermal bremsstrahlung and synchrotron radiation, and at high frequencies, to the thermal radio emission of interstellar dust. The frequency range between 40 and 85 GHz, where the contribution from galactic sources is minimal, is found to be optimal for CMB studies.

The working frequency of Relikt-1 is marked in Fig. 3 by an asterisk. Clearly, this frequency is close to the optimal range.

The use of a single frequency in Relikt-1 significantly simplified the experiment, but could strongly complicate the interpretation of the results. However, the WMAP data evidence that at this frequency, the anisotropy is more than 75% due to CMB radiation. Therefore, the single-frequency measurements of Relikt-1 are quite relevant.

Of course, this conclusion is valid only for an initial search experiment, which is what Relikt-1 was. Subsequent more detailed and precise CMB experiments, undoubtedly, require multi-frequency observations. This is realized in the COBE, WMAP, and Planck experiments.

### 10. Conclusion

The data obtained by the WMAP satellites have a high signal-to-noise ratio. This allows using them to estimate the quality of other CMB observations carried out at the frequency range from 20 to 100 GHz with a large angular resolution of one degree or more. The analysis of the mutual covariance of data

allows reliably estimating the results of observations even with a poor signal-to-noise ratio. Such an analysis was applied to the Relikt-1 data and showed that at a 98% confidence level, the signal discovered by Relikt-1 corresponds to the actual CMB anisotropy. The cold spot found on the Relikt-1 map was also confirmed.

The author thanks A A Brukhanov for the useful discussions. The work used LAMBDA (Legacy Archive for Microwave Background Data Analysis) data [13]. Part of the results was obtained using the HEALPix program [14] and the IDL Astronomy Library [15].

## References

1. Strukov I A et al. *Pis'ma Astron. Zh.* **18** 387 (1992) [*Astron. Lett.* **18** 153 (1992)]
2. Smoot G F et al. *Astrophys. J.* **396** L1 (1992)
3. Strukov I A et al. *Pis'ma Astron. Zh.* **13** 163 (1987) [*Astron. Lett.* **13** 65 (1987)] [Translated into English: Strukov I A et al., JPRS Report. Science & Technology. USSR: Space (1987) p. 59]
4. Bennett C L et al. *Astrophys. J.* **414** L77 (1993)
5. Banday A J *Lecture Notes Phys.* **429** 111 (1994)
6. Wilkinson Microwave Anisotropy Probe, <http://wmap.gsfc.nasa.gov>
7. Cruz M et al. *Astrophys. J.* **655** 11 (2007)
8. Cayon L, Smoot G *Astrophys. J.* **452** 487 (1995)
9. Hinshaw G *Astrophys. J. Suppl.* **170** 288 (2007)
10. Bennett C L et al. *Astrophys. J. Suppl.* **148** 1 (2003)
11. Legacy Archive for Microwave Background Data Analysis: WMAP TT Power Spectra, [http://lambda.gsfc.nasa.gov/product/map/dr3/pow\\_tt\\_spec\\_get.cfm](http://lambda.gsfc.nasa.gov/product/map/dr3/pow_tt_spec_get.cfm)
12. Strukov I A, Skulachev D P, in *Itogi Nauki i Tekhniki. Ser. Astronomiya* (Science and Technics Itogi. Ser. Astronomy) Vol. 31 (Moscow: VINITI, 1986) p. 37
13. Legacy Archive for Microwave Background Data Analysis: WMAP Five Year Smoothed Stokes I Sky Maps Per Differencing Assembly, [http://lambda.gsfc.nasa.gov/product/map/dr3/maps\\_da\\_smth\\_r9\\_i\\_5yr\\_get.cfm](http://lambda.gsfc.nasa.gov/product/map/dr3/maps_da_smth_r9_i_5yr_get.cfm)
14. HEALPix, <http://healpix.jpl.nasa.gov>
15. The IDL Astronomy User's Library, <http://idlastro.gsfc.nasa.gov>